

9. R. Boeschl, *Nature (London)* **236**, 25 (1972).
10. W. Born and F. Begemann, *Earth Planet. Sci. Lett.* **25**, 159 (1975).
11. J. DeFelice, G. G. Fazio, E. L. Fireman, *Science* **142**, 673 (1963).
12. L. A. Rancitelli, R. W. Perkins, J. A. Cooper, J. H. Kaye, N. A. Wogman, *ibid.* **166**, 1269 (1969).
13. R. W. Perkins, L. A. Rancitelli, J. A. Cooper, J. H. Kaye, N. A. Wogman, *ibid.* **167**, 577 (1970).
14. P. J. Cressy and D. D. Bogard, *Geochim. Cosmochim. Acta* **40**, 749 (1976).
15. I. R. Cameron and Z. Top, *ibid.* **39**, 1705 (1975).
16. E. J. Olsen, A. Norman, K. Fredriksson, E. Jarosewich, G. Moreland, *Meteoritics* **13**, 209 (1978).
17. T. Kirsten, D. Ries, E. L. Fireman, *ibid.*, in press.
18. We thank W. A. Cassidy for the four Allan Hills meteorite samples. This research was supported in part by NASA grants NGR 09-015-145 and NAS 9-11712.

1 November 1978; revised 15 December 1978

Sea-Level Fluctuations and Deep-Sea Sedimentation Rates

Abstract. *Sediment accumulation rate curves from 95 drilled cores from the Pacific basin and sea-level curves derived from continental margin seismic stratigraphy show that high biogenous sediment accumulation rates correspond to low eustatic sea levels for at least the last 48 million years. This relationship fits a simple model of high sea levels producing lower land/sea ratios and hence slower chemical erosion of the continents, and vice versa.*

A preliminary study based on sediment thickness (*l*) indicates that there have been large-scale fluctuations in the average sedimentation rate in the major ocean basins and that these fluctuations are synchronous and global in extent. In that study, rates were expressed in meters per million years and were uncorrected for compaction with increasing burial depth. Consequently, in this analysis, younger and less compacted sediments appear to have higher sedimentation rates than older, more compacted ones, even though the total flux of material to the sea floor might have remained constant. We have therefore recalculated Pacific Ocean sedimentation rates in terms of mass per unit area per unit time (grams per square centimeter per 10^3 years) in the manner suggested by van Andel *et al.* (2) for both total accumulation rate and carbonate accumulation rate. The basic data are taken from the published *Initial Reports of the Deep Sea Drilling Project* (3) and from the files of the DSDP data base in La Jolla, California.

The procedure used in calculating sedimentation rates is relatively simple (4). Basically, it consists of determining the age (in years) of every level below the sea floor at each location and then using compositional and porosity data to calculate the total mass and bulk composition of the sediment that has accumulated at each locality during a particular time interval. In this study we used 3-million-year time increments. The results shown in Fig. 1a are simple arithmetic averages from 95 sites in the Pacific Ocean.

Figure 1a also compares the results from the two methods of expressing the Pacific Ocean sedimentation rates. The recalculated data do not refute the basic

conclusion of the earlier study of Davies *et al.* (1) that the ocean apparently alternates between periods of high and low sedimentation, but there are significant changes in the relative amplitudes and sometimes the phase of the fluctuations. For instance, the ratio of the total sedimentation rate in the latest Pliocene and Quaternary (0 to 3 million years) to that in the Upper Oligocene (24 to 27 million years) is about 5:1 as calculated by Davies *et al.* (1) and only 2:1 in the present recalculation. Similarly, the carbonate sedimentation rate ratios obtained by the two methods are 3:1 and 1:2, respectively, for the same two intervals. Although such differences may be due in

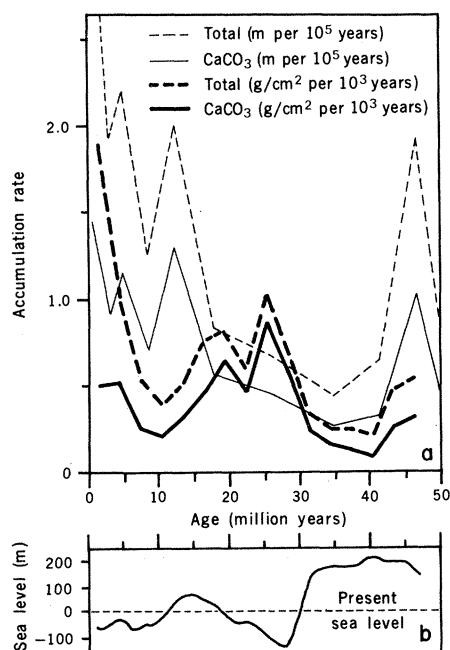


Fig. 1. (a) Pacific Ocean sedimentation rates from (1) and this report. (b) Eustatic sea-level changes (5). The time scale for both (a) and (b) is from (5).

part to the slightly inequivalent time intervals used to average the rates in the studies, it is clear that they are mainly due to differential compaction. We therefore believe that our curve represents the best currently available estimate of the Pacific Ocean sediment accumulation rate through time.

Figure 1 shows that the sedimentation rates are correlated with the global sea-level fluctuations postulated by Vail *et al.* (5), with high accumulation rates occurring at times of low sea level and vice versa. This correlation is especially significant because the sea-level curve was derived from continental-shelf seismic data and sea-floor spreading rates and, therefore, is completely independent of the data base used in calculating the oceanic sedimentation rates. In constructing Fig. 1b we modified the sea-level curve by sampling it at 0.5-million-year intervals and smoothing it by using a seven-point moving average in order to compare it with our results, which were calculated for 3-million-year intervals. Furthermore, as the sediment accumulation curve was quantitatively calculated from deep-sea core data and the sea-level curve was interpreted from seismic data, we have more confidence in the phase than in the amplitude correlation of the two.

As pointed out by Rona (6), a correlation between sea level and sedimentation rate suggests that at times of high sea level, material eroded from the continents is trapped on the continental shelves. During times of low sea level the shelf sediments are exposed, and previously deposited shelf sediment is weathered and eroded. The resulting erosion products are then flushed to the deep sea. However, order-of-magnitude calculations (7, 8) suggest that the continental erosion rates are so high and the shelf so small that some material must almost always bypass the shelf.

Because of the limited drainage area of the Pacific basin and the fact that the deep Pacific is surrounded by trenches, which prevent bottom transport of continental detritus (9), we propose that the sea level-sedimentation rate correlation represents mainly biogenous precipitates (carbonate and opal) and not erosional detritus. In this model, high sea levels allow high rates of biogenous precipitation on the shelves, thus starving the ocean basins, whereas low sea levels permit dissolved river loads to reach the deep sea and foster chemical erosion of material to the seafloor might have remained contrast, the detrital load of rivers always enters the ocean at point sources

on the continental margins, which rapidly prograde to the shelf edge during rising sea levels, leaving large portions of the submerged shelf free to accumulate carbonate. During low sea levels, detritus completely bypasses the shelves, so that clastic sediments almost always accumulate continuously in the continental rises.

If Pacific Ocean accumulation rates represent mainly flux of dissolved carbonate and silica, one might expect a positive correlation between high sea level and carbonate compensation depth (CCD), as suggested by Berger and Winterer (7). However, this correlation is weak at present. Berger (10) noted some similarities between sea level and the CCD for the Cenozoic, but the question of whether sea level and the CCD are coupled remains open because of the difficulty of accurately calculating the Cenozoic history of the CCD.

The suggestion of Davies *et al.* (1) that fluctuations in the input of land-derived material to the deep oceans are related to alternating rates of continental erosion and that these are a consequence of alternating climatic states remains plausible. However, until more detailed estimates are available of the amount of material in the different reservoirs of the geochemical system and of the changing fluxes between the reservoirs, it will not be possible to determine to what extent input of land-derived material to the deep sea is a function of the land/ocean ratio, which is in turn a function of sea level, and to what extent climatic factors influencing continental erosion rates may be involved. We suggest, as have Fisher and Arthur (11), that climate itself is a function of the land/ocean ratio and thus a function of sea level. Thus climate, sea level, and deep-ocean sediment accumulation have a complex dynamic relationship, many details of which remain to be investigated.

THOMAS R. WORSLEY

Department of Geology,
Ohio University,
Athens 45701

THOMAS A. DAVIES

Department of Geology,
Middlebury College,
Middlebury, Vermont 05753

References and Notes

1. T. A. Davies, W. W. Hay, J. R. Southam, T. R. Worsley, *Science* **197**, 53 (1977).
2. Tj. H. van Andel, G. R. Heath, T. C. Moore, *Geol. Soc. Am. Mem.* **143** (1975).
3. *Initial Reports of the Deep Sea Drilling Project* (Government Printing Office, Washington, D.C., 1969-1976), vols. 5-9, 16-21, and 30-32.
4. T. R. Worsley and T. A. Davies, *Mar. Geol.*, in press.
5. P. R. Vail, R. M. Michum, S. Thompson III, in *Seismic Stratigraphy—Applications to Hydrocarbon Exploration*, C. E. Payton, Ed. (American

6. Association of Petroleum Geologists, Tulsa, Okla., 1977), pp. 83-97.
7. P. Rona, *Nature (London)* **244**, 25 (1973).
8. W. H. Berger and E. L. Winterer, in *Pelagic Sediments on Land and Under the Sea*, K. J. Hsu and H. C. Jenkyns, Eds. (Blackwell, Oxford, 1974), pp. 11-48.
9. W. W. Hay and J. R. Southam, in *The Fate of Fossil Fuel CO₂ in the Oceans*, N. R. Anderson and A. Malahoff, Eds. (Plenum, New York, 1977), pp. 569-604.
10. H. W. Menard, *Marine Geology of the Pacific* (McGraw-Hill, New York, 1964).
11. W. H. Berger, in *The Fate of Fossil Fuel CO₂ in the Oceans*, N. R. Anderson and A. Malahoff,

Eds. (Plenum, New York, 1977), pp. 505-542.

12. A. G. Fisher and M. L. Arthur, *Soc. Econ. Paleontol. Mineral. Spec. Publ.* **25** (1977), pp. 19-51.
13. The Deep Sea Drilling Project is supported by the National Science Foundation and operated by Scripps Institution of Oceanography with advice from the Joint Oceanographic Institution. We thank P. Woodbury and C. Suchland for their aid in obtaining the data in appropriate format and for their advice. This work was supported by NSF grants OCE-75-04066 and OCE-76-81934.

15 September 1978

Manganese Oxide Tunnel Structures and Their Intergrowths

Abstract. *Natural hollandite and romanechite are widespread barium-containing manganese minerals. High-resolution transmission electron microscopy indicates that intergrowths of the two minerals occur in a coherent manner on the unit-cell level with no apparent ordering of the hollandite and romanechite. Other structures have been imaged that are based on the hollandite and romanechite structures. Electron microscopy holds a key to unraveling the myriad structural complexities of the manganese oxides.*

The oxides of Mn are large in number and complex in character; many of their structures are poorly known. The difficulties associated with distinguishing between them and the extent of intimate mixing that occurs have given rise to the descriptive but intentionally imprecise names of "wad" for the soft oxides and "psilomelane" for the hard, massive, botryoidal variety (1). This report will focus on hollandite, $\sim\text{BaMn}_8\text{O}_{16}$, and mixtures containing hollandite and romanechite, $\sim(\text{Ba}_2\text{H}_2\text{O})_4\text{Mn}_{10}\text{O}_{20}$ (2).

Hollandite and romanechite, two of the more common psilomelane oxides, occur in sediments, weathered outcrops, the supergene zone of Mn and base metal ore deposits, and metamorphosed Mn deposits. The hollandite structure itself is of interest because it is the form as-

sumed by K, Sr, and Ba feldspars at high pressures, such as occur within the earth's mantle (3).

Our primary method of study has been high-resolution transmission electron microscopy (HRTEM), both by direct structure imaging and by selected area diffraction. These techniques have shown that coherent intergrowths occur between hollandite and romanechite. These intergrowths may account (i) for the reported range in compositions between different hollandites and romanechites and (ii) for the variable and problematical x-ray patterns obtained from romanechite samples (4).

The hollandite and romanechite structures can be placed in a structural classification of Mn oxides that is somewhat analogous to the system developed for rock-forming silicates (5). The $(\text{SiO}_4)^{4-}$ tetrahedron has its counterpart in the $(\text{MnO}_6)^{8-}$ octahedron of MnO_2 minerals. The octahedra share corners and edges to form chain, framework, or sheet structures. The single-chain structure is pyrolusite ($\beta\text{-MnO}_2$), and the double-chain structure is ramsdellite (Mn_2O_3). Hollandite has a framework structure consisting of double chains of Mn octahedra joined at roughly right angles so as to have a nearly square pattern (2×2) when viewed down the length of chains (Fig. 1a). Romanechite is closely related, with a 3×2 , nearly rectangular arrangement of $(\text{MnO}_6)^{8-}$ chains (Fig. 1b). A variety of large mono- and divalent cations such as K, Na, Ba, Sr, and Pb can then be accommodated within the square or rectangular tunnels thus formed (6).

We studied samples from three localities. We analyzed each sample by (i) x-ray powder diffraction, using a Guinier

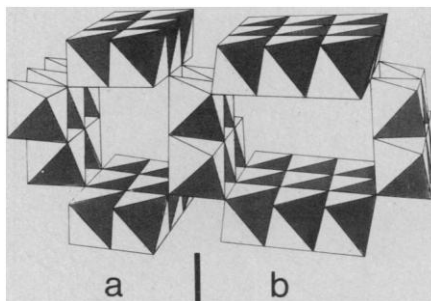


Fig. 1. Schematic of a hollandite-romanechite intergrowth. Each octahedron represents a Mn cation surrounded by six O atoms. (a) Hollandite with its double chains of Mn octahedra. The chains form a square cross section (2×2) when viewed down the tunnel length. (b) Romanechite with its 3×2 rectangular cross section. The double chain is common to both structures and is the basis for unit-cell intergrowths. The tunnels formed in both structures accommodate the large Ba cations or substituting cations.